Improving the Power Efficiency of a PV Power Generation System Using a Proposed Electrochemical Heat Engine Embedded in the System

Hassan Fathabadi

***Abstract*—An important issue in the photovoltaic (PV) power generation systems is the massive amount of heat wasted by PV modules/panels. For the first time, this paper provides a new solution to recover a portion of the mentioned waste heat by utilizing a proposed electrochemical heat engine. A thermally regenerative electrochemical cycle (TREC) system has been designed, constructed, and embedded in a PV power generation system including a 200-W PV module to harvest the waste heat of its PV module, so a PV-TREC hybrid system has been organized and built. The hot cell of the TREC system has been positioned in direct contact with the backside of the PV module, and the cold cell is in direct contact with a heat sink located in the shade of the PV module. Experimental verifications demonstrate that the proposed TREC system efficiently converts the waste heat into electric power ranging from 0.1 to 54.5 W. In this manner, up to 6% of the waste heat of the PV module is recovered. It also substantiated that the daily energy efficiency of the PV-TREC hybrid system is improved by 27.5% compared to a usual PV system, and this is the main contribution and novelty of this paper.**

***Index Terms*—Electrochemical heat engine, photovoltaic (PV) power generation systems, PV-thermally regenerative electrochemical cycle (PV-TREC) hybrid system.**

NOMENCLATURE

A	Surface area of the electrodes of cells (cm^2).
$D_{\rm pv}$	Duty cycle of the PV converter.
$D_{\rm trec}$	Duty cycle of the TREC converter.
$E_{\rm pv-trec}$	Daily energy production of the PV-TREC system.
$E_{\rm pv}$	Daily energy production of the PV system.
F	Faraday's constant (96 485.3 C mol^{-1}).
G	Solar irradiance on the PV module surface ($W \cdot m^{-2}$).
i	Current density circulating between cells ($A \cdot cm^{-2}$).
I	Electric current circulating between cells (A).
$I_{\rm load}$	Electric current supplied to the inverter (A).

Manuscript received May 29, 2018; revised July 9, 2018, August 20, 2018, September 26, 2018, and October 4, 2018; accepted November 12, 2018. Date of publication November 28, 2018; date of current version June 10, 2019. Recommended for publication by Associate Editor J. A. Cobos. *(Corresponding author: Hassan Fathabadi.)*

The author is with the School of Electrical and Computer Engineering, National Technical University of Athens, 10682 Athens, Greece (e-mail:

Rankine cycle (ORC) [1], dual-loop ORC [2], Kalina cycle [3], and heat-pipe technique [4] are some samples of such thermodynamic cycles. To make the heat conversion process more efficient, a combination of two or more thermodynamic cycles can also be utilized [5], [6]. Different types of thermoelectric materials are available [7], which convert heat into electricity, but their output powers as well as their efficiencies are low [8]. This point makes them inappropriate to be utilized in most industrial applications [9]. In an electrochemical heat engine, two electrochemical reactions are performed at two different temperatures. Because of the difference between the energy levels of the two electrochemical reactions, a net electric energy occurs [10]. Thermally regenerative electrochemical cycle (TREC) is an electrochemical heat engine [11]. The TREC was utilized to harvest low-grade heat energy and the outcome of the research showed that a conversion efficiency of 5.7% is achievable [12]. In another research, a low-cost membrane-free TREC system with the conversion efficiency of 3.5% was proposed [13]. It was shown that for a charging-free TREC system operating in the temperature range of 20–60 °C, a conversion efficiency of 2% is attainable [14]. The impact of finite heat transfer and environmental factors on the power production of a TREC system was evaluated using finite time analysis [15]. A system composed of a proton exchange membrane fuel cell and a TREC system was designed to recover the heat losses of the system, and the efficiency of the system was improved by 2.74%–8.27% [16]. Optimization of the parameters of the TREC system was carried out to maximize its output power [17].

The enormous amount of heat wasted by the photovoltaic (PV) modules is an important issue. This paper addresses this issue by embedding the proposed TREC system in a PV power generation system to form a PV-TREC hybrid system. The proposed TREC system has been constructed and the experimental results substantiate the contribution of this research work in harvesting up to 6% of the waste heat of the PV module, and improving the daily energy efficiency of the PV-TREC hybrid system by 27.5%. The TREC and a TREC-based system are analyzed in detail in Section II. The details of the proposed TREC system and the constructed PV-TREC hybrid system together with relevant experimental verifications are given in Section III, and the paper is concluded in Section IV.

II. Theoretical Concepts of a TREC-Based System

A TREC cell is composed of two electrodes, positive and negative, separated by an anion membrane. In a TREC cell, four processes (steps) occur in a sequence in time: Heating up (Step 1), charging (Step 2), cooling down (Step 3), and discharging (Step 4) as shown in Fig. 1. There is a difference between two voltages charged in the two electrodes of the TREC cell during charging as shown in Fig. 1. As a result, an electric power is produced by the TREC cell during discharging (Step 4). Solid CuHCF immersed in 6M $NaNO_3$ aqueous solution is used to build the positive electrode, and the negative electrode is constructed by utilizing copper immersed in 3M $Cu(NO_3)_2$ aqueous

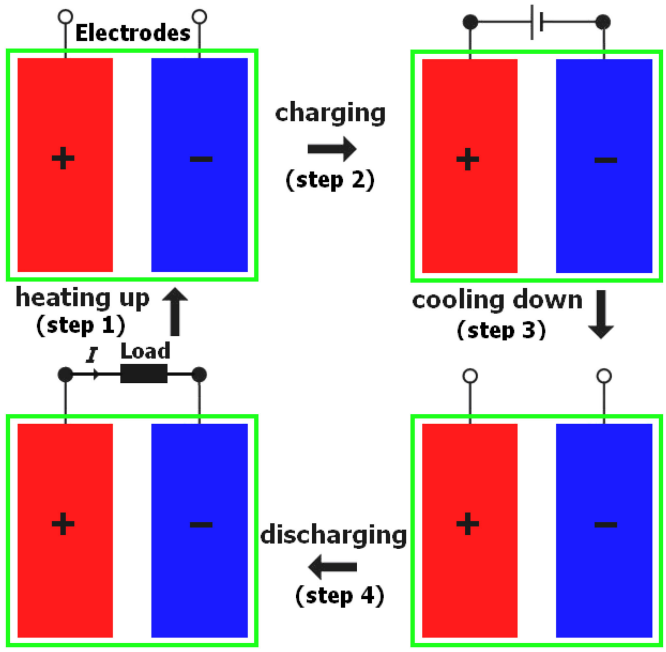

Fig. 1. Four processes performed in a TREC cell.

solution [17]. During charging, chemical reactions occurring in the two electrodes are as follows:

$$\begin{cases} \text{Positive electrode} : 2\,\text{Na} \rightarrow 2\,\text{Na}^{+} + 2e \\ \text{Positive electrode} : 2\,\text{Na}^{+} + 2\text{NO}^{-}{}_{3} \rightarrow 2\,\text{NaNO}_3 \\ \text{Negative electrode} : \text{Cu}(\text{NO}_3)_2 \rightarrow \text{Cu}^{+2} + 2(\text{NO}_3^{-}) \\ \text{Negative electrode} : \text{Cu}^{+2} + 2e \rightarrow \text{Cu}. \end{cases} \tag{1}$$

During discharging, the direction of these chemical reactions reverses to produce electric current as follows:

$$\begin{cases} \text{Negative electrode} : \text{Cu} \rightarrow \text{Cu}^{+2} + 2e \\ \text{Negative electrode} : \text{Cu}^{+2} + 2(\text{NO}^{-}{}_{3}) \rightarrow \text{Cu}(\text{NO}_3)_2 \\ \text{Positive electrode} : 2\text{NaNO}_3 \rightarrow 2\text{Na}^{+} + 2\text{NO}^{-}{}_{3} \\ \text{Positive electrode} : 2\text{Na}^{+} + 2e \rightarrow 2\text{Na}. \end{cases} \tag{2}$$

The system proposed in this study operates based on the TREC and consists of two TREC cells; a hot cell positioned in the higher temperature part of the system, and a cold cell located in the lower temperature part as shown in Fig. 2. As a result, a net energy resulting from the difference between charging and discharging energies is extracted from the system during discharging, and a portion of the waste heat of the system is recaptured. In a TREC system including hot and cold cells, the isothermal coefficient of each cell is defined as follows:

$$\alpha_c = \left(\frac{\partial V_{\text{oc}}}{\partial T}\right)\Big|_{\substack{T=T_n \\ \text{iso. process}}} = \frac{\Delta \dot{s}}{nF}. \tag{3}$$

Using (3), the open-circuit voltage of the hot cell is formulized as

$$V_{\text{oc-hot}} = \alpha_c T_H = \frac{\Delta \dot{s}}{nF} T_H. \tag{4}$$

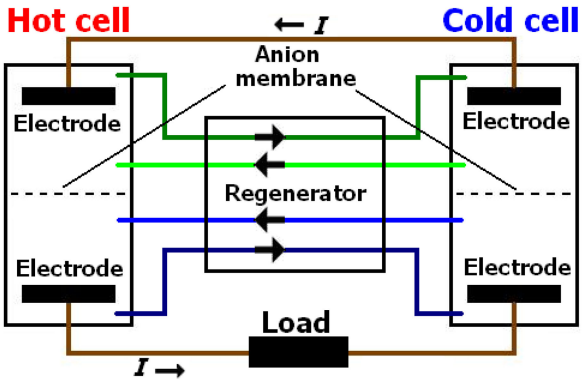

Fig. 2. Configuration of a system operating based on the TREC.

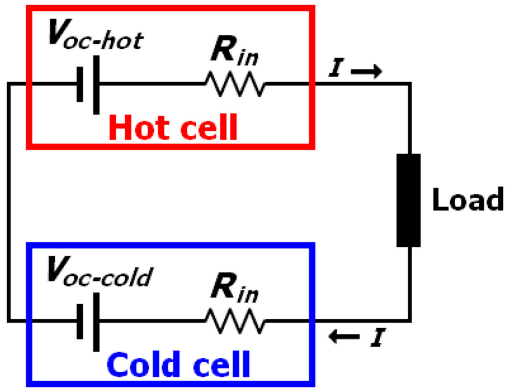

Fig. 3. Equivalent circuit of the embedded TREC system.

The rate of the heat absorbed by the hot cell is composed of two portions. The first portion, which is reversible and provided by the waste heat of the system, is given as

$$\dot{Q}_H = T_H\,\Delta\dot{S}_H = \alpha_c\, I\, T_H. \tag{5}$$

The second portion is the heat loss resulting from the regeneration that is expressed as

$$\Delta\dot{Q}_{\mathrm{re}_H} = c_p\dot{\eta}_H(1-\eta_{\mathrm{re}})(T_H - T_L). \tag{6}$$

The power loss caused by the electric current (I) flowing through the internal resistance of the hot cell occurs as heat loss and its rate is calculated as

$$\dot{Q}_{\mathrm{loss}} = \frac{dQ_{\mathrm{loss}}}{dt} = R_{\mathrm{in}}I^2. \tag{7}$$

Considering the above-mentioned points and using (5)–(7), the rate of the total heat absorbed by the hot cell is obtained as

$$\begin{aligned}\dot{Q}_{H_{\mathrm{tot}}} &= \dot{Q}_H + \Delta\dot{Q}_{\mathrm{re}_H} - \dot{Q}_{\mathrm{loss}}\\ &= \alpha_c I T_H + c_p\dot{\eta}_H(1-\eta_{\mathrm{re}})(T_H - T_L) - R_{\mathrm{in}}I^2.\end{aligned} \tag{8}$$

Using (3), the open-circuit voltage of the cold cell is obtained as

$$V_{\mathrm{oc-cold}} = \alpha_c T_L = \frac{\Delta\, \dot{s}}{nF}T_L. \tag{9}$$

Similarly, the rate of the heat released by the cold cell is composed of two portions. The first portion is reversible and is given as

$$\dot{Q}_L = T_L\,\Delta\dot{S}_L = \alpha_c I T_L. \tag{10}$$

The chemical reactions occurring during the discharging process are regenerated by passing ions NO_3^- through the anion membrane separating the positive and negative electrodes. The second portion is the heat loss resulting from this regeneration that is expressed as

$$\Delta\dot{Q}_{\mathrm{re}_L} = c_p\dot{\eta}_L(1-\eta_{\mathrm{re}})(T_H - T_L). \tag{11}$$

The heat loss of the cold cell's internal resistance is given as

$$\dot{Q}_{\mathrm{loss}} = \frac{dQ_{\mathrm{loss}}}{dt} = R_{\mathrm{in}}I^2. \tag{12}$$

Using (10)–(12), the rate of the total heat released by the cold cell is obtained as

$$\begin{aligned}\dot{Q}_{L_{\mathrm{tot}}} &= \dot{Q}_L + \Delta\dot{Q}_{\mathrm{re}_L} + \dot{Q}_{\mathrm{loss}}\\ &= \alpha_c I T_L + c_p\dot{\eta}_L(1-\eta_{\mathrm{re}})(T_H - T_L) + R_{\mathrm{in}}I^2\end{aligned} \tag{13}$$

where $\dot{\eta}_H$ is the molar flow rate of the electrolyte solution in the hot cell and is defined as

$$\dot{\eta}_H = \frac{I}{F\varphi_H}. \tag{14}$$

Similarly, $\dot{\eta}_L$ is the molar flow rate of the electrolyte solution in the cold cell and is defined as

$$\dot{\eta}_L = \frac{I}{F\varphi_L}. \tag{15}$$

The molar percentage of the reactant in the electrolyte solution in the hot cell (φ_H) equals to that of the cold cell (φ_L), so

$$\dot{\eta}_H = \dot{\eta}_L. \tag{16}$$

Now, the net electric power produced by the TREC system is found by subtracting the rate of the total heat released by the cold cell from the rate of the total heat absorbed by the hot cell as shown in the following:

$$P_{\mathrm{out}} = \dot{Q}_{H_{\mathrm{tot}}} - \dot{Q}_{L_{\mathrm{tot}}} = \alpha_c I(T_H - T_L) - 2R_{\mathrm{in}}I^2. \tag{17}$$

By substituting (4) and (9) in to (17), it can be rewritten as

$$P_{\mathrm{out}} = (V_{\mathrm{oc-hot}} - V_{\mathrm{oc-cold}})I - 2R_{\mathrm{in}}I^2. \tag{18}$$

Using (18), the equivalent circuit of the TREC system is obtained in detail as shown in Fig. 3. To evaluate the efficiency of the TREC system, its conversion (power) efficiency is calculated as

$$\gamma = \frac{P_{\mathrm{out}}}{\dot{Q}_{H_{\mathrm{tot}}}} = \frac{\alpha_c I(T_H - T_L) - 2R_{\mathrm{in}}I^2}{\alpha_c I T_H + c_p\dot{\eta}_H(1-\eta_{re})(T_H - T_L) - R_{\mathrm{in}}I^2}. \tag{19}$$

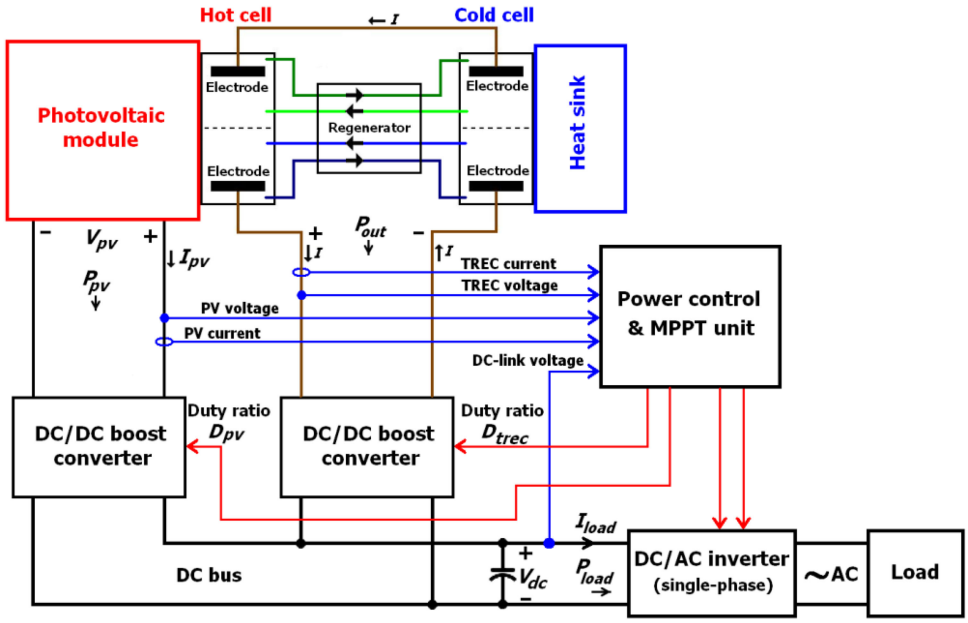

Fig. 4. Proposed system: Configuration of the constructed PV-TREC hybrid system.

III. Proposed TREC System Embedded in a PV System and Experimental Verifications

In this research, to recover the waste heat produced by a PV module, a TREC system has been designed, built, and embedded in a usual PV power generation system to form a PV-TREC hybrid system, the configuration of which is shown in detail in Fig. 4. The usual PV system is composed of a PV module and a dc/dc boost converter so that its duty cycle is continuously regulated to extract maximum power from the PV module by a maximum power point tracking (MPPT) controller located in a unified power control and MPPT unit as shown in Fig. 4. A modified incremental-conductance technique reported in [18], which is also applicable to wind and fuel cell systems [19], [20], has been utilized to implement the MPPT controller. The TREC system comprises of two hot and cold cells connected to the dc bus via a dc/dc boost converter of which the duty cycle is continuously regulated by the unified power control and MPPT unit to adjust the dc-link voltage to a designated constant voltage. As shown in Fig. 4, the hot cell of the TREC system has been positioned in direct contact with the backside of the PV module, while the cold cell is in direct contact with a heat sink located in the shade of the PV module. Based on the configuration shown in Fig. 4, the PV-TREC hybrid system has been constructed to provide experimental verifications. A detailed photo of the constructed TREC system positioned on the backside of the PV module is shown in Fig. 5, and the electric circuit of the constructed PV-TREC hybrid system is shown in detail in Fig. 6. The detailed parameters of the constructed TREC system embedded in the PV system together with the technical specifications of all the components used to construct the PV-TREC hybrid system have been summarized in Table I. As reported in Table I and shown in Fig. 6, two similar dc/dc boost converters each having an output capacitance of 22 μF

Fig. 5. Photo of the constructed TREC system positioned on the backside of the PV module.

have been connected to the dc bus, so a capacitance of 680 μF, which is high enough to provide a dc-link voltage of 100 V with negligible ripple has been chosen for the dc-link capacitor. All the details of the two similar boost converters used to construct PV-TREC hybrid system have been reported in [21]. All the experiments and measurements relevant to this research have been performed in Athens. As reported in Table I, a PV module KC200GT has been utilized in the constructed PV-TREC hybrid system. Point-by-point measurements demonstrate that when the PV module is in operation, the temperature of the hot cell (T_H), which is in direct contact with it, ranges from 28 to 92 °C on a sunny day in summer, while the associated temperature of the cold cell (T_L), which is in direct contact with the heat sink ranges from 23 to 41 °C. This means that the difference between the temperatures of the two cells ranges from 5 to 51 °C, i.e., $(T_H - T_L) \in [5\,^{\circ}\mathrm{C}, 51\,^{\circ}\mathrm{C}]$. To measure the electrical parameters of the constructed TREC system, the converter connected to the TREC system was disconnected, and the difference

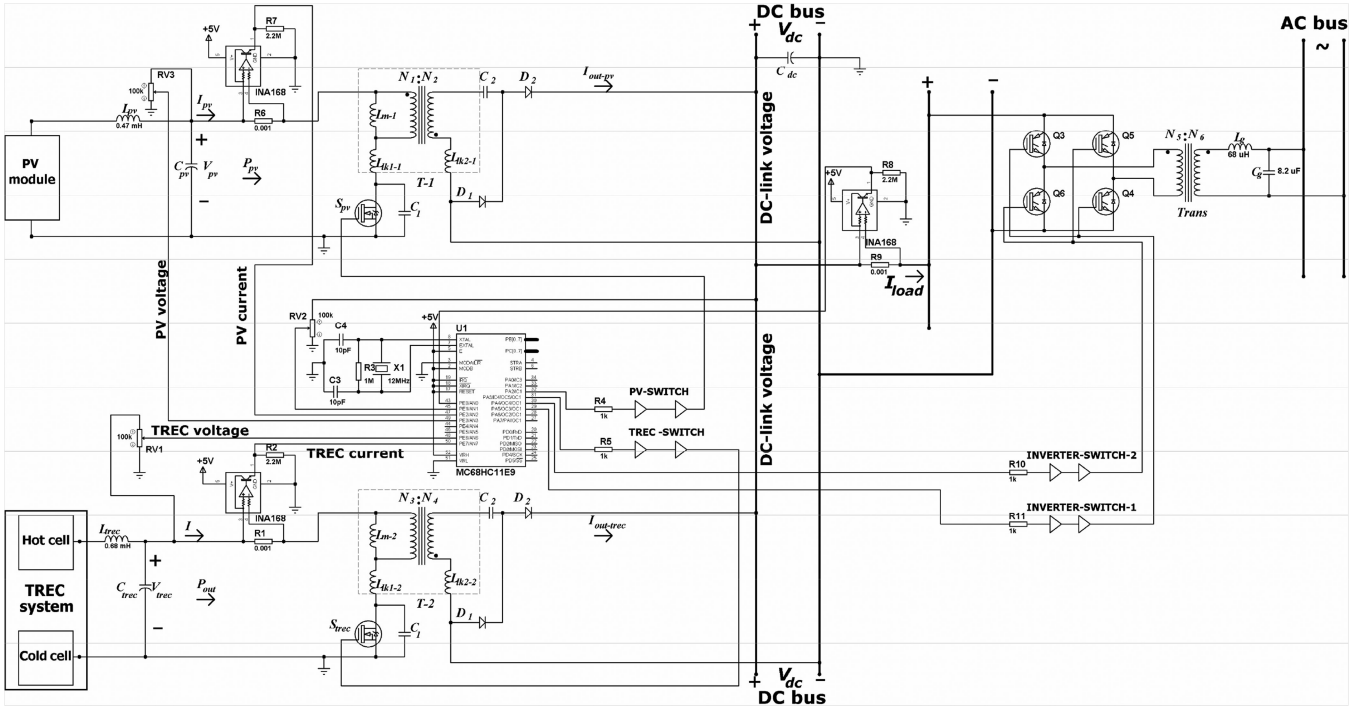

Fig. 6. Electric circuit of the constructed PV-TREC hybrid system.

TABLE I
TECHNICAL SPECIFICATIONS OF THE COMPONENTS USED TO CONSTRUCT THE PV-TREC HYBRID SYSTEM

TREC system		**Two DC/DC boost converters connected to the PV module and TREC system**	
T_H (K)	301-365	C_{pv} (μF) and C_{trec} (μF)	470 and 220
T_L (K)	296-314	Switching frequency: f_s (kHz)	25
α_c (VK^{-1})	1.22×10^{-3}	DC-link voltage V_{dc} (V)	100
η_{re}	0.74	DC-link capacitor C_{dc} (μF)	680
γ (%) and γ_{ave} (%)	0.2-6 and 3.1	ESR of C_{dc}: R_{esr} (mΩ)	109
A (cm^2)	50×30	C_2 (μF) and C_1 (nF)	22 and 1.2
Weight (kg)	3.1	N_2 / N_1	25/15
PV module KC200GT (under STC)		N_4 / N_3	675/2
Current at MPP (A)	7.61	MOSFET switch S_{pv} & S_{trec}	IRFPS40N60K
Voltage at MPP (V)	26.3	Diodes: D_1 - D_2	15ETH06S
Output power at MPP (W)	200.1430	**Single-phase inverter**	
Open-circuit voltage (V)	32.9	IGBT switches: Q3-Q6	STGY40NC60VD
Short-circuit current (A)	8.21	N_6 / N_5	32/20
Length × Width × Depth (mm)	$1425\times990\times36$	L_g (μH) and C_g (μF)	68 and 8.2

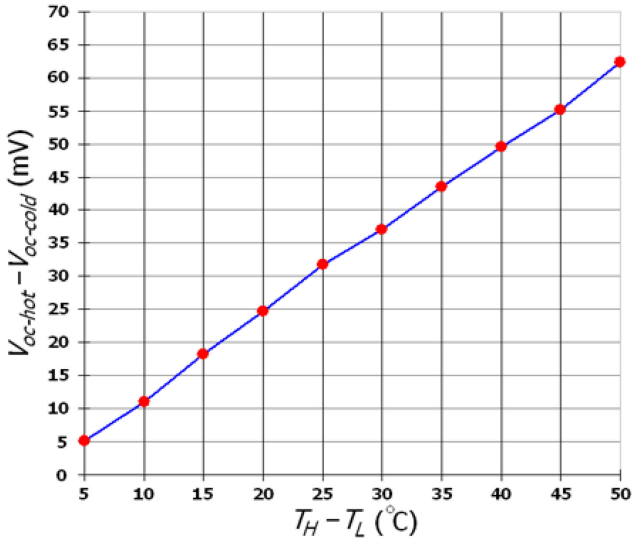

Fig. 7. Difference between the open-circuit voltages of the hot and cold cells.

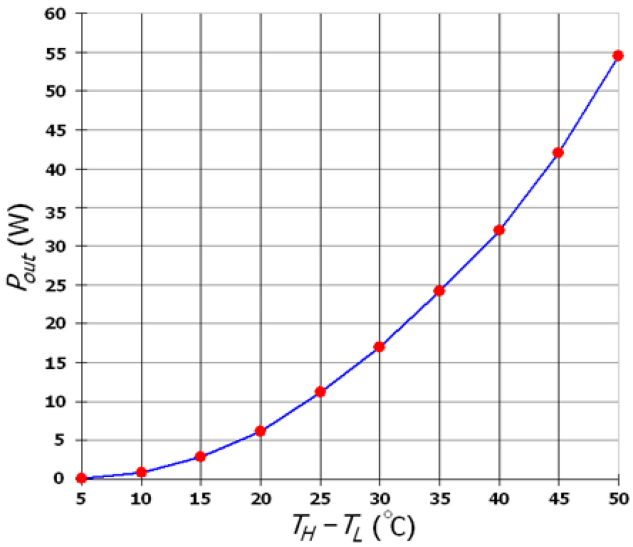

Fig. 9. Output electric power of the embedded TREC system.

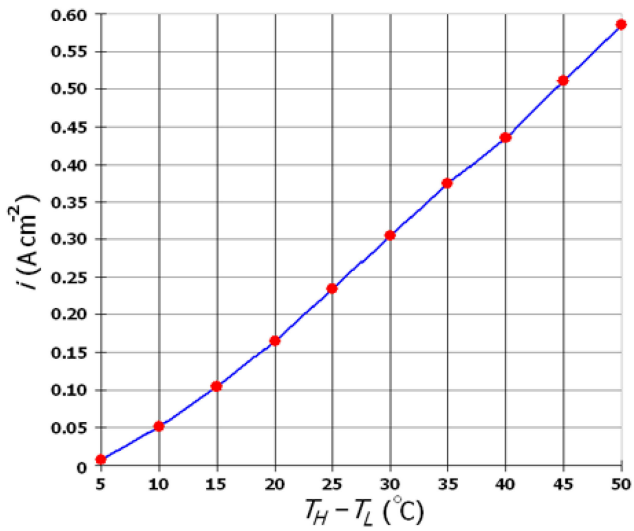

Fig. 8. Density of the current circulating between the hot and cold cells.

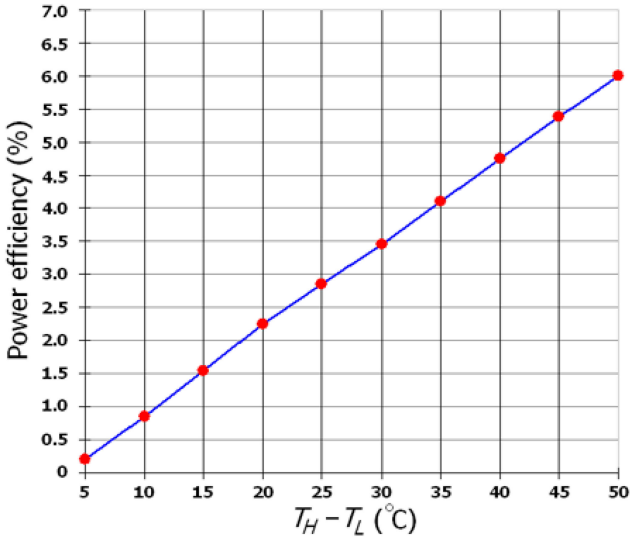

Fig. 10. Power efficiency of the embedded TREC system.

between the open-circuit voltages of the hot and cold cells ($V_{\mathrm{oc-hot}} - V_{\mathrm{oc-cold}}$) was measured point by point in the temperature range of 5–50 °C using a digital voltmeter and the measurement results are shown as a curve in Fig. 7. The hot and cold cells were connected to each other through a digital ampere meter, and the electric current circulating between the two cells was measured point by point in the temperature range of 5–50 °C. Then, the measured data were divided by the surface areas of the electrodes used in the hot and cold cells (A) to calculate the current density, which is shown in Fig. 8. The TREC system was connected to a variable resistor and the output electric power of the TREC system was measured point by point in the temperature range of 5–50 °C using a digital wattmeter and the measured data are shown in Fig. 9. It can be seen that the electric power production of the TREC system ranges from 0.1 to 55 W, so the average power production is 27.3 W. Finally, the power efficiency of the TREC system was calculated point by point in the temperature range of 5–50 °C by substituting the output power and current of the TREC system measured point by point in (19). The calculated power efficiency that ranges from 0.2% to 6% in the temperature range of 5–50 °C is shown in Fig. 10. The power–efficiency curve explicitly demonstrates that the TREC system provides an average conversion efficiency of about 3.1%. This means that on an average, about 3.1% of the waste heat of the PV module is recovered by the proposed TREC system embedded in the PV power generation system. Since the TREC system provides a maximum power efficiency of 6% in the temperature range of 5–50 °C, up to 6% of the waste heat can also be recaptured. It can be summarized that on average, the TREC system embedded in the PV-TREC hybrid system acts as an electrochemical power source with the average capacity of 0.027 kWh, this means that after each 37 h, 1 kWh of electric energy is produced by the constructed TREC system that is a considerable amount of electric energy obtained by

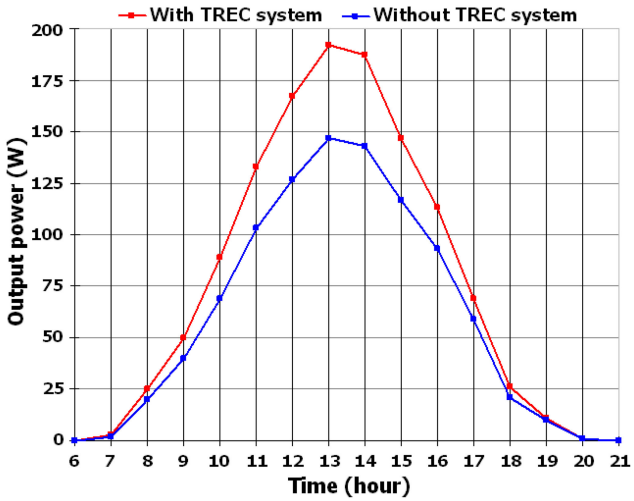

Fig. 11. Output power of the PV system with and without the proposed TREC system.

only recapturing a portion of the waste heat of the PV module. The cost of the TREC system and the converter connected to it is about 125 euros. Comparing this cost with the technical and environmental benefits (producing 1 kWh per 37 h by recovering waste heat and keeping the earth's temperature lower) obtained by utilizing the TREC system technically and economically justifies the utilization of the proposed TREC system. An experiment was performed on a sunny day in spring, when ambient temperature ranged from 16 to 28 °C, to measure the daily energy production of the constructed PV-TREC hybrid system in two modes: First, the TREC system is in operation (PV-TREC hybrid mode), and second, the TREC system is OFF (PV mode). In other words, the experiment was performed to measure the daily energy production of the PV system with and without the proposed TREC system. Measurements were performed hour by hour such that the results have been shown as two hour-by-hour curves in Fig. 11. The measured data demonstrated that the daily energy production of the PV-TREC hybrid system is about 1.213 kWh (the area under the red curve), while the daily energy production of the PV system without the TREC system (usual PV system) is about 0.952 kWh (the area under the blue curve). Thus, improvement in the daily energy efficiency of the constructed PV-TREC hybrid system compared to a usual PV system can be calculated as

$$\frac{\gamma_{\mathrm{pv-trec}}}{\gamma_{\mathrm{pv}}} = \frac{E_{\mathrm{pv-trec}}}{E_{\mathrm{pv}}} \times 100 = \frac{1.213}{0.952} \times 100 \approx 127.5\%. \tag{20}$$

This means that the daily energy efficiency of the PV-TREC hybrid system on a sunny day in spring has been improved by 27.5% compared to a usual PV system, and this is the main contribution and novelty of this research work. Enhancement of the daily energy efficiency is more than 27.5% on a sunny day in summer because of further increase in the PV-module temperature. On a sunny day in autumn, environmental conditions are similar to spring, so the enhancement of the daily energy efficiency can be considered same as that in spring, i.e., about 27.5%. Enhancement of the daily energy efficiency is less than 27.5% on a sunny day in winter because the PV module temperature is not high enough, and so, the power production of the TREC system is less than that in spring, summer, and autumn. Considering the above-mentioned explanation, it can be summarized that the average enhancement of the daily energy efficiency of the constructed PV-TREC hybrid system compared to a usual PV system is about 27.5% on a sunny day. During a cloudy day the PV module is shaded, so the temperatures of the PV module and heat sink are close to each other, and also close to ambient temperature, as a result, the power production of the TREC system is almost zero. Considering this point, enhancement of annual energy efficiency of the constructed PV-TREC hybrid system compared to a usual PV system can be estimated as

$$\text{Enhancement of annual energy efficiency} = \frac{\text{Number of sunny days a year}}{365} \times 27.5\%. \tag{21}$$

The two converters connected to the PV module and TREC system operate under zero-current switching (ZCS) and zero-voltage switching (ZVS) conditions. The transformer used in the converter connected to the PV module is a pulse transformer with turns ratio $N_2/N_1 = 25/15$. It has been realized by utilizing a Mn–Zn ferrite EI core 0T49928EC made by Magnetics Co., and enameled copper round wire used in the primary and secondary windings with the diameter of 2.0320 and 1.0160 mm, respectively. As reported in Table I, the output voltage and current of the PV module KC200GT supplied to the primary winding change in the range of 0–32.9 V and 0–8.21 A, respectively. The voltage of the secondary winding connected to the dc bus is 100 V, and its current ranges from 0 to 2 A. As reported in Table I, a pulse transformer with turns ratio $N_4/N_3 = 675/2$ has been used in the converter connected to the TREC system. It has been realized by utilizing one Mn–Zn ferrite UU core PC40 UU100 × 151 × 30 made by TDK Co., four sets of parallel-connected enameled copper rectangular wire 5.6 mm × 16 mm with the current rating of 227.62 A made by CMP Controls Pty. Ltd. used in the primary winding, and enameled copper round wire with the diameter of 0.5080 mm used in the secondary winding. The output voltage, current, and power of the TREC system supplied to the converter connected to it range up to 62.7 mV, 877.5 A, and 55 W, respectively. The voltage of the secondary side connected to the dc bus is 100 V, and its current is below 0.45 A. The two-pulse transformers operate based on LLC resonant topology and achieve ZVS and ZCS over their operating range [21]. The converter connected to the PV module provides a power efficiency of 94.92% over its input operating range of 200 W as shown in Fig. 12. Similarly, the power efficiency of the converter connected to the TREC unit ranges up to 73.78% when its input power changes up to a range of 55 W as shown in Fig. 13.

The primary purity of the positive electrode (CuHCF) and negative electrode (Cu) used in the constructed TREC system is about 98%. The purity declines over time due to depositions and reaches about 60% when the internal resistance of each cell

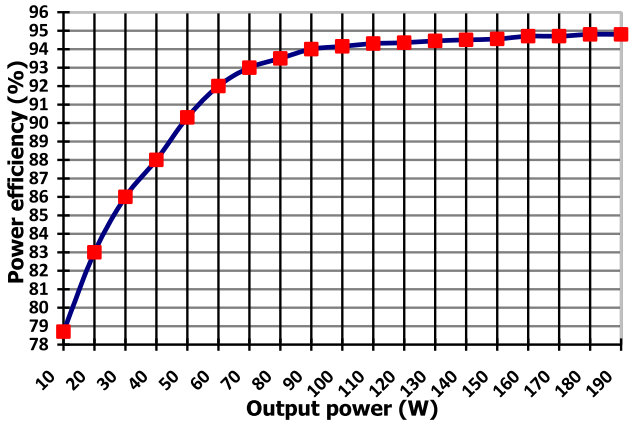

Fig. 12. Experimental measurement: Efficiency of the converter connected to the PV module.

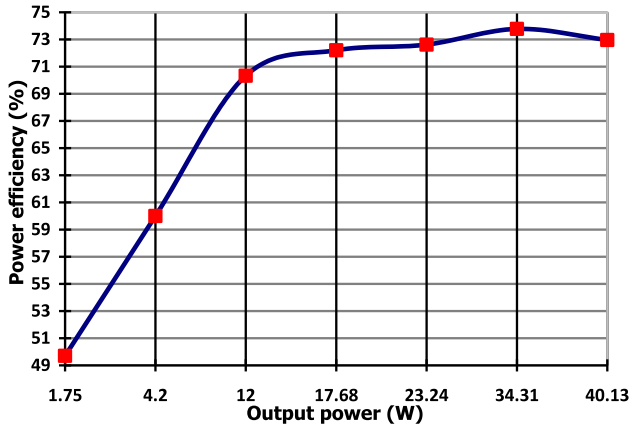

Fig. 13. Experimental measurement: Efficiency of the converter connected to the TREC unit.

increases, and the electrodes and electrolyte should be replaced. The average lifetime of the electrodes and electrolyte of the constructed TREC system is about 4 years.

IV. Conclusion

In this study, a portion of the waste heat of a PV module was recovered by embedding the proposed TREC system in a PV system to form a PV-TREC hybrid system. The experimental results relevant to the constructed PV-TREC hybrid system were given that not only demonstrated that the TREC system efficiently converts the waste heat of the PV module into electric power, but also substantiated the novelty of this research work by harvesting up to 6% of the waste heat and improving the daily energy efficiency of the PV-TREC hybrid system by 27.5% compared to a usual PV system. It is also clear that the lifetime of the TREC system is less than that of a PV module.

References

[1] R. Long, Y. J. Bao, X. M. Huang, and W. Liu, "Exergy analysis and working fluid selection of organic Rankine cycle for low grade waste heat recovery," *Energy*, vol. 73, pp. 475–483, 2014.

[2] T. Li, J. Zhu, K. Hu, Z. Kang, and W. Zhang, "Implementation of PDORC (parallel double-evaporator organic Rankine cycle) to enhance power output in oilfield," *Energy*, vol. 68, pp. 680–687, 2014.

[3] W. Fu, J. Zhu, T. Li, W. Zhang, and J. Li, "Comparison of a Kalina cycle based cascade utilization system with an existing organic Rankine cycle based geothermal power system in an oilfield," *Appl. Therm. Eng.*, vol. 58, no. 1/2, pp. 224–233, 2013.

[4] A. Franco and M. Vaccaro, "On the use of heat pipe principle for the exploitation of medium-low temperature geothermal resources," *Appl. Therm. Eng.*, vol. 59, no. 1/2, pp. 189–199, 2013.

[5] X. Meng, F. Bai, F. Yang, Z. Bao, and Z. Zhang, "Study of integrated metal hydrides heat pump and cascade utilization of liquefied natural gas cold energy recovery system," *Int. J. Hydrogen Energy*, vol. 35, no. 13, pp. 7236–7245, 2010.

[6] T. Li, J. Zhu, and W. Zhang, "Cascade utilization of low temperature geothermal water in oilfield combined power generation, gathering heat tracing, and oil recovery," *Appl. Therm. Eng.*, vol. 40, pp. 27–35, 2012.

[7] L. E. Bell, "Cooling, heating, generating power, and recovering waste heat with thermoelectric systems," *Science*, vol. 321, no. 5895, pp. 1457–1461, 2008.

[8] F. J. DiSalvo, "Thermoelectric cooling and power generation," *Science*, vol. 285, no. 5428, pp. 703–706, 1999.

[9] T. M. Tritt and M. Subramanian, "Thermoelectric materials, phenomena, and applications: A bird's eye view," *MRS Bull.*, vol. 31, no. 3, pp. 188–198, 2006.

[10] H. Fathabadi, "Solar energy harvesting in buildings using a proposed novel electrochemical device as an alternative to PV modules," *Renewable Energy*, vol. 133, pp. 118–125, 2018.

[11] H. Fathabadi, "Internal combustion engine vehicles: Converting the waste heat of the engine into electric energy to be stored in the battery," *IEEE Trans. Veh. Technol.*, vol. 67, no. 10, pp. 9241–9248, Oct. 2018.

[12] S. W. Lee *et al.*, "An electrochemical system for efficiently harvesting low-grade heat energy," *Nature Commun.*, vol. 5, 2014, Art. no. 3942.

[13] Y. Yang *et al.*, "Membrane-free battery for harvesting low-grade thermal energy," *Nano Lett.*, vol. 14, no. 11, pp. 6578–6583, 2014.

[14] Y. Yang *et al.*, "Charging-free electrochemical system for harvesting low-grade thermal energy," *Proc. Nat. Acad. Sci.*, vol. 111, no. 48, pp. 17011–17016, 2014.

[15] R. Long, B. Li, Z. Liu, and W. Liu, "Ecological analysis of a thermally regenerative electrochemical cycle," *Energy*, vol. 107, pp. 95–102, 2016.

[16] R. Long, B. Li, Z. Liu, and W. Liu, "A hybrid system using a regenerative electrochemical cycle to harvest waste heat from the proton exchange membrane fuel cell," *Energy*, vol. 93, pp. 2079–2086, 2015.

[17] Y. Wang, L. Cai, W. Peng, Y. Zhou, and J. Chen, "Maximal continuous power output and parametric optimum design of an electrochemical system driven by low-grade heat," *Energy Convers. Manage.*, vol. 138, pp. 156–161, 2017.

[18] H. Fathabadi, "Novel fast dynamic MPPT (maximum power point tracking) technique with the capability of very high accurate power tracking," *Energy*, vol. 94, pp. 466–475, 2016.

[19] H. Fathabadi, "Plug-in hybrid electric vehicles (PHEVs): Replacing internal combustion engine with clean and renewable energy based auxiliary power sources," *IEEE Trans. Power Electron.*, vol. 33, no. 11, pp. 9611–9618, Nov. 2018.

[20] H. Fathabadi, "Combining a proton exchange membrane fuel cell (PEMFC) stack with a Li-ion battery to supply the power needs of a hybrid electric vehicle," *Renewable Energy*, vol. 130, pp. 714–724, 2019.

[21] H. Fathabadi, "Novel high efficiency dc/dc boost converter for using in photovoltaic systems," *Solar Energy*, vol. 125, pp. 22–31, 2016.

Hassan Fathabadi was born in Tehran in 1969. He received the B.S., M.S., and Ph.D. degrees in electrical engineering from Polytechnic University, Tehran, Iran, in 1992, 1997, and 2002, respectively.

From 2009 to 2012, he was a Postdoctoral Researcher with the National Technical University of Athens, Athens, Greece, where he is currently working as a Professor. He is the sole author of more than 75 papers published in high-ranking ISI journals and 30 inventions. His research interests include power electronics, microelectronics, control, mechatronics, energy conversion, transmission lines, and power systems.